Nano Energy 26 (2016) 164–171

Contents lists available at ScienceDirect

Nano Energy

journal homepage: www.elsevier.com/locate/nanoen

Hybridized nanogenerator for simultaneously scavenging mechanical and thermal energies by electromagnetic-triboelectric-thermoelectric effects

Xue Wang [a], Zhong Lin Wang [a,b,*], Ya Yang [a,*]

[a] Beijing Institute of Nanoenergy and Nanosystems, Chinese Academy of Sciences; National Center for Nanoscience and Technology, Beijing 100083, China
[b] School of Materials Science and Engineering, Georgia Institute of Technology, Atlanta, Georgia 30332-0245, United States

ARTICLE INFO

Article history:
Received 15 March 2016
Received in revised form
16 May 2016
Accepted 19 May 2016
Available online 20 May 2016

Keywords:
Nanogenerator
Hybridized
Thermoelectric
Electromagnetic
Triboelectric

ABSTRACT

High-efficiency rotation based energy harvesters require simultaneous scavenging of mechanical energy and rotation-induced wasted thermal energy. A hybridized nanogenerator is reported that has an electromagnetic generator (EMG), a triboelectric nanogenerator (TENG), and a thermoelectric generator (ThEG) for simultaneously harvesting mechanical and thermal energies in one process. As driven by the relative rotation motions between two disks, all of the EMG, TENG and ThEG can deliver outputs due to the cooperative operation of electromagnetic, triboelectric, and thermoelectric effects. With increasing the working time of the hybridized nanogenerator, the output power of EMG can be kept in a stable value, and an obvious increase can be seen for the output power of ThEG, while the output power of TENG exhibited a dramatic decrease. By using the power management circuits, all of the EMG, TENG, and ThEG devices can deliver a constant output voltage of 5 V, where the hybridized nanogenerator can produce a pulsed output current peak of about 160 mA. Moreover, the hybridized nanogenerator has been successfully installed in a commercial bicycle to scavenge biomechanical energy for lighting up globe lights and charging up a cell phone.

1. Introduction

Due to the challenges of energy crisis and environmental issues, more and more efforts have been impelled in looking for renewable energies in the environment to realize sustainable development of modern society [1–3]. As one of the most commonly available energies, mechanical energy has been successfully converted into electricity by some energy harvesting devices, such as electromagnetic generators (EMGs) [4,5], piezoelectric nanogenerators [6–8], and triboelectric nanogenerators (TENGs) [9–11]. Among them, TENGs have several obvious advantages of light weight, low cost, and high output power [12–16], which can be utilized to scavenge almost all forms of mechanical energies, where the rotation motions can result in the largest output power of the TENG due to high frequencies [17]. Previous investigation has indicated that a large energy loss exists in the TENG due to the friction induced heat dissipation [18], where the triboelectric effect-induced waste thermal energy can be dramatically increased in the TENG with increasing the working time of the device, especially for the high-speed rotation based TENGs. The using of a thermoelectric generator (ThEG) to scavenge the waste thermal energy is an ideal solution to minimize the energy loss in the TENG. Although the EMG has been integrated in the rotation based TENG to increase the total output power of the device [14,19], there has been no any report about the efficient integration of TENG and ThEG.

Here, we have developed a hybridized nanogenerator that can simultaneously scavenge mechanical and thermal energies due to the cooperative operation of electromagnetic, triboelectric, and thermoelectric effects. Both the EMG and TENG can deliver output voltage/current signals under the relative rotation motions between two disks. Moreover, the triboelectric effect-induced waste thermal energy can be scavenged by using a ThEG. By using the power management circuits, all the EMG, TENG, and ThEG devices can deliver a constant DC output voltage of 5 V, where the output current peak of the hybridized nanogenerator can be up to about 160 mA. Moreover, we also demonstrated that the fabricated hybridized nanogenerator can be installed in a commercial bicycle for scavenging the human motions induced biomechanical energy to drive some electronic devices or charge a cell phone.

* Corresponding author at: Beijing Institute of Nanoenergy and Nanosystems, Chinese Academy of Sciences, National Center for Nanoscience and Technology, Beijing 100083, China.
E-mail addresses: zlwang@gatech.edu (Z.L. Wang), yayang@binn.cas.cn (Y. Yang).

http://dx.doi.org/10.1016/j.nanoen.2016.05.032
2211-2855/

2. Experimental section

2.1. Fabrication of the hybridized nanogenerator

The fabricated hybridized nanogenerator includes an EMG, a TENG and a ThEG. The EMG consists of eight magnets (the diameter of 25 mm and the thickness of 1.8 mm for each one) and the corresponding eight coils (the diameter of 25 mm, the thickness of 1.2 mm, and the coil turns of about 2000), where the eight magnets with a magnetic alternating means have been set in a circular acrylic disk. The TENG includes a layer of radial-arrayed Cu strips as a triboelectric material, a layer of polyamide film (the diameter of 14.5 cm, the thickness of 50 μm) as another triboelectric material, and two sets of complementary radial-arrayed Cu electrodes, where a layer of protection layer was utilized to prevent the oxidation of Cu electrodes. The polyamide film was fixed on the protection layer. The relative rotation motions between the Cu strips and the polyamide film can drive the working of the TENG, resulting in the observed output voltage/current signals. The ThEG is composed of eight thermoelectric units with the dimensions of 4 cm × 4 cm × 0.4 cm with the connection in series. When the TENG is working, the triboelectric effect-induced thermal energy can increase the temperature for one side of ThEG, where the produced temperature difference between the two sides of the ThEG can drive the working of the ThEG.

3. Results and discussion

Fig. 1(a) presents a schematic diagram of the fabricated hybridized nanogenerator, where the device consists of a rotator and a stator. The EMG consists of eight magnets (layer 1) with the magnetic poles in alternating arrangement in an acrylic disk and eight groups of coils (layer 5) in series connection at the corresponding positions of the magnets. The TENG consists of the radially-arrayed sectors (layers 2 and 4) and the triboelectric material (polyamide film) at the middle section (layer 3), where the layer 3 was fixed on the layer 4. The ThEG is fixed in the stator (layer 6) to scavenge the waste thermal energy. Fig. 1(b) shows six optical images of the layers 1–6, indicating that the diameter of the EMG and TENG is about 14.5 cm. As displayed in Fig. 1(c), the photograph of the hybridized nanogenerator illustrates that the hybridized nanogenerator can work under relative rotation motions between the rotator and the stator.

Fig. 2(a) displays the electricity generation process of the EMG under the relative rotation motions between the rotator and the

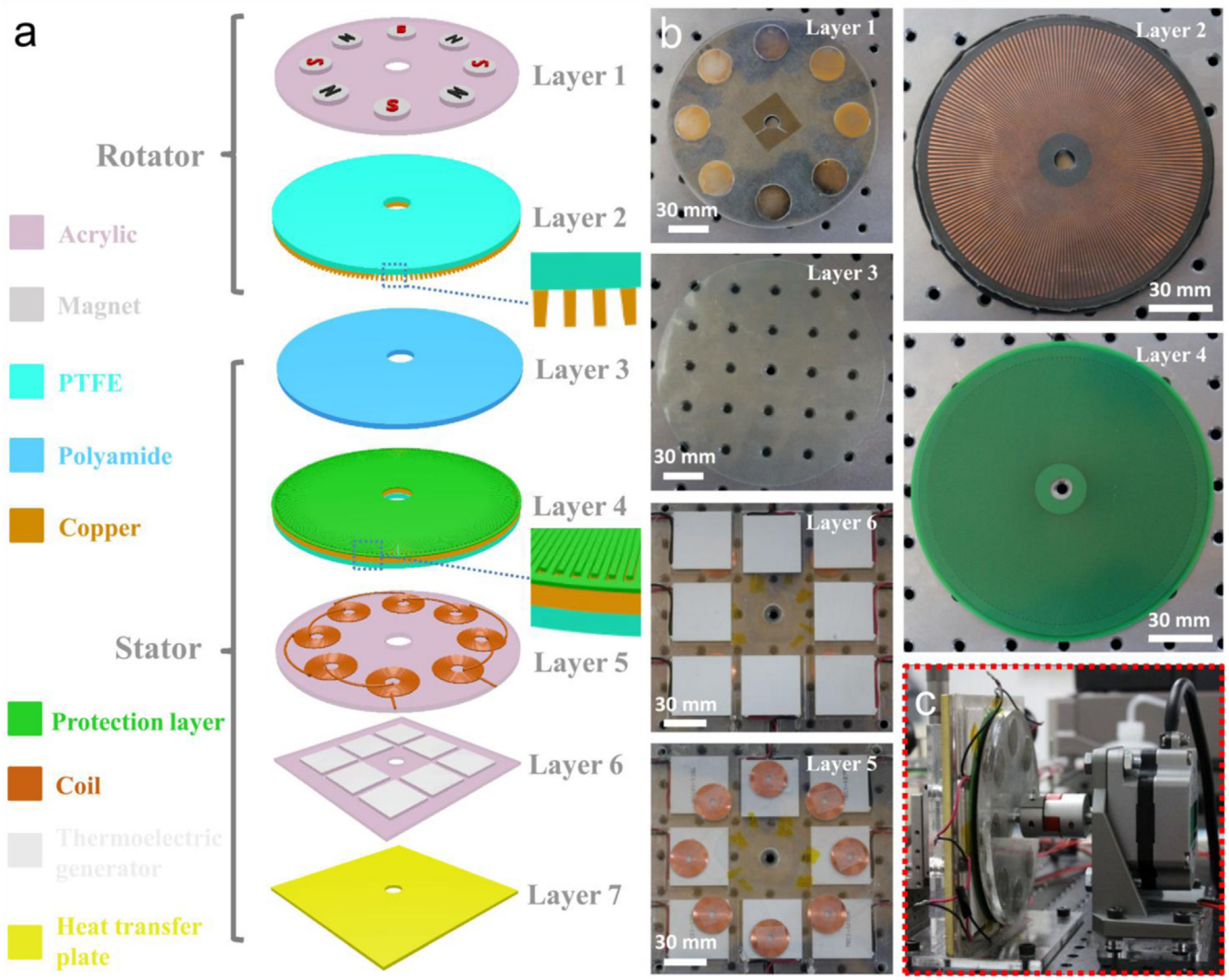

Fig. 1. (a) Schematic diagram of the fabricated hybridized nanogenerator. (b) Photographs of the hybridized nanogenerator with the different layers. (c) Photograph of the hybridized nanogenerator.

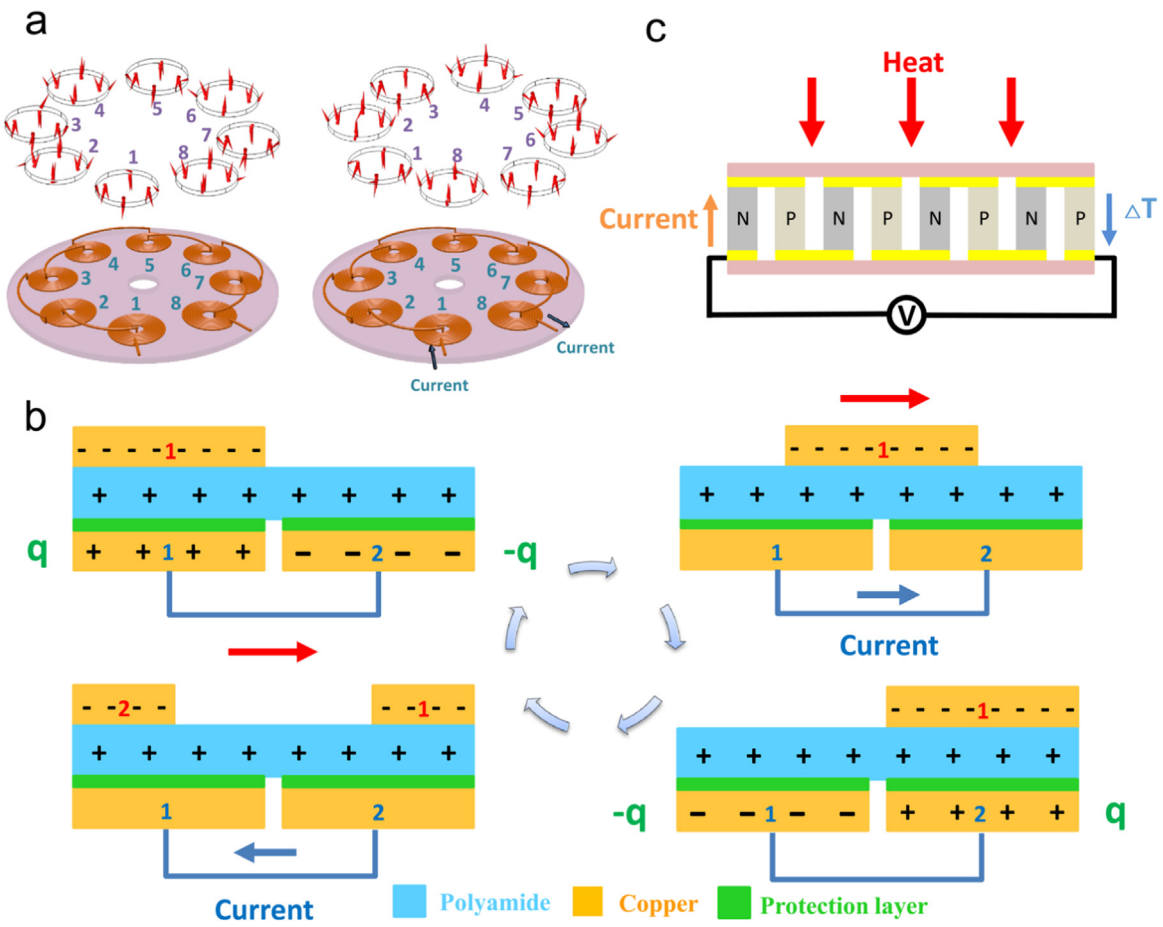

Fig. 2. (a) Schematic diagram of the working principle for the EMG under the relative rotation between the magnets and the coils. (b) Schematic diagram of the working principle for the TENG under the relative rotation between the Cu strips and the polyamide film. (c) Schematic diagram of the working principle for the ThEG.

stator. The output voltage/current signals of EMG can be observed when the magnetic flux through the coils changes under a relative rotation motion between the magnets and the coils. Fig. 2 (b) illustrates the working process of the TENG. Under the relative rotation motions between the Cu gratings on the rotator and the polyamide film on the stator, the electrons can be injected from polyamide film to Cu according to the different triboelectric polarities. At the initial status, the Cu grating-1 is at the top position of the Cu electrode-1, resulting in that the negative and positive charges can be created on the two Cu electrodes due to the electrostatic induction effect. When the Cu grating-1 was moved from the bottom Cu electrode-1 to Cu electrode 2, the electrons can flow from electrode 2 to electrode 1, resulting in the observed voltage/current signals between the two electrodes. The working of the TENG is based on the electrons flow between the two electrodes due to the relative motion-induced charge unbalance on the two Cu electrodes. Fig. 2(c) illustrates the working principle of the ThEG. Under the relative rotation motions between the rotator and the stator, the temperature can increase at the interface of the TENG, resulting in a temperature difference between the two sides of the ThEG. Both the electrons and holes can be moved from the hot side to the cold side, inducing an output voltage/current of the ThEG.

As depicted in Fig. 3(a), the EMG delivers an output current of about 4.5 mA and an output voltage of about 26.5 V under the rotation speed of 1000 r/min. Fig. 3(b) presents that the output current and voltage of the TENG can be up to 3.6 mA and 58.7 V, respectively. Fig. 3(c) displays that both the output current and voltage of the ThEG can increase with increasing the working time of the device, where the current and voltage can be up to 57.7 mA and 1.2 V after the device is working in about 220 s, respectively. Peaks of the output voltages are associated with the triboelectric process between the rotator and the stator. To understand the output characteristics of the different energy harvesting unit, the impedances of the devices have been investigated by measuring the output current signals under the different loading resistances. Fig. 3(d) illustrates that the output current of the EMG decreases with increasing the loading resistances, resulting in a largest output power of about 26.5 mW under the loading resistance of about 6 kΩ. As presented in Fig. 3(e), the output current of the TENG exhibited an obvious decrease with increasing the loading resistance, where the largest output power of the TENG is about 238.9 mW under a loading resistance of about 40 kΩ. Fig. 3 (f) displays that the output current of the ThEG increases with increasing the working time of the device under a loading resistance of 30 Ω, where a largest output power of about 14.5 mW can be realized after the device was working for 280 s To compare output performances of the EMG and the TENG, the produced electricity can be calculated by using the current data under the condition of the largest output power. As illustrated in Fig. 3(g), the produced electricity energy of the EMG is about 0.2 mJ in 15 ms, which is much smaller than that of the TENG (1.8 mJ) in 15 ms, as shown in Fig. 3(h). Fig. 3(i) shows the temperature difference at the two sides of the ThEG when the device is working, indicating that the fabricated ThEG can be utilized to effectively scavenge the waste thermal energy from the mechanical rotation motions.

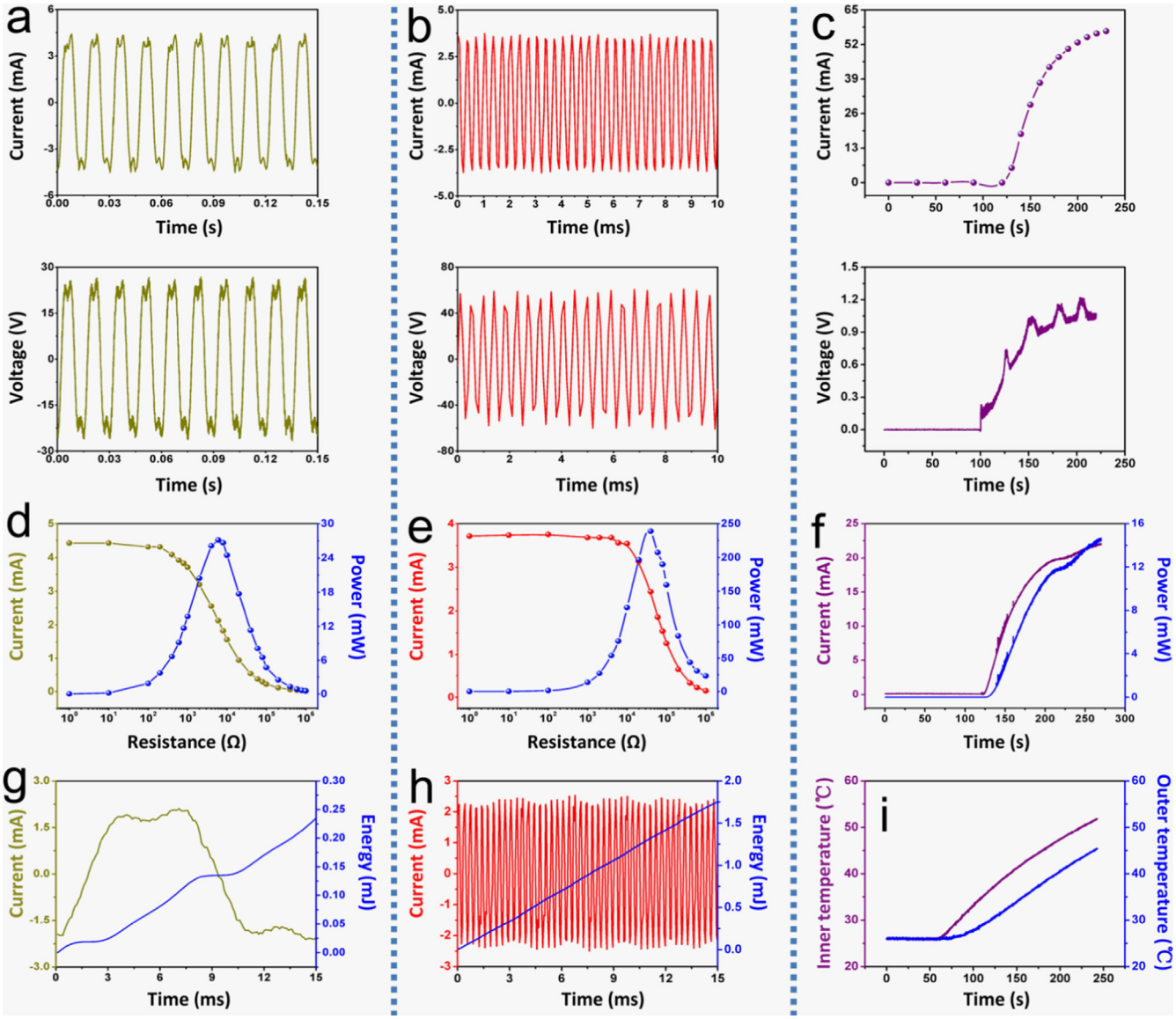

Fig. 3. (a, b, c) Output current and voltage signals of the EMG (a), TENG (b), and ThEG (c). The rotation speed is 1000 r/m. (d, e, f) Output current and the corresponding power signals of the EMG (d), TENG (e), and ThEG (f). The current curve of ThEG was measured under a loading resistance of 30 Ω. (g, h) The enlarged output current and the produced electric energy of the EMG (g) and TENG (h). (i) The temperature changing curves at the two sides of the ThEG.

Fig. 4(a) illustrates the output voltage and current of the EMG under the different rotation rates, indicating that both the output voltage and current of the EMG increase with increasing the rotation rates. Under the rotation speed of 3000 r/min, the output voltage and current of the EMG can be up to 72.9 V and 11.4 mA, respectively. For the TENG, the output current increases with increasing the rotation rates, while the output voltage under a loading resistance of 1 MΩ decreases with increasing the rates, as presented in Fig. 4(b). As shown in Fig. 4(c), the power of the EMG also increases with increasing the rotation rates, where it can be up to 187.9 mW under the rotation speed of 3000 r/min. The impendence of the EMG keeps at a constant value of 6 kΩ under the different rotation rates. With increasing the rotation rate to 3000 r/min, the power of the TENG can be increased to 572.1 mW, while the corresponding impendence of the TENG decreases with increasing the rotation rates, as depicted in Fig. 4(d). Under a rotation speed of 3000 r/min, the impendence of the TENG is about 8 kΩ, which is very close to that of the EMG (6 kΩ), indicating that the impendence matching for the TENG and EMG can be achieved by increasing the rotation rates.

As displayed in Fig. 4(e), under a rotation rate of 3000 r/min, the output current of the EMG with the loading resistance of 6 kΩ exhibits a constant value of about 2.1 mA with increasing the working time of the device, resulting in a constant power of about 26.5 mW. However, a dramatic decrease for the output current and power of the TENG under a loading resistance of 40 kΩ can be clearly seen in Fig. 4(f). After the TENG was working for 180 s, the corresponding output power has been decreased from 224.4 mW to 47.9 mW. To compare the output performances of the three energy harvesting units further, the average output power $P_{average}$ of the device can be expressed as

$$P_{average} = \frac{\int_{t_1}^{t_2} I^2 \cdot R dt}{t_2 - t_1} \quad (1)$$

where I is the output current of the device under the loading resistance of R, t_1 and t_2 are the selected times of the calculation. For the EMG, the corresponding average output power $P_{average}$ is about

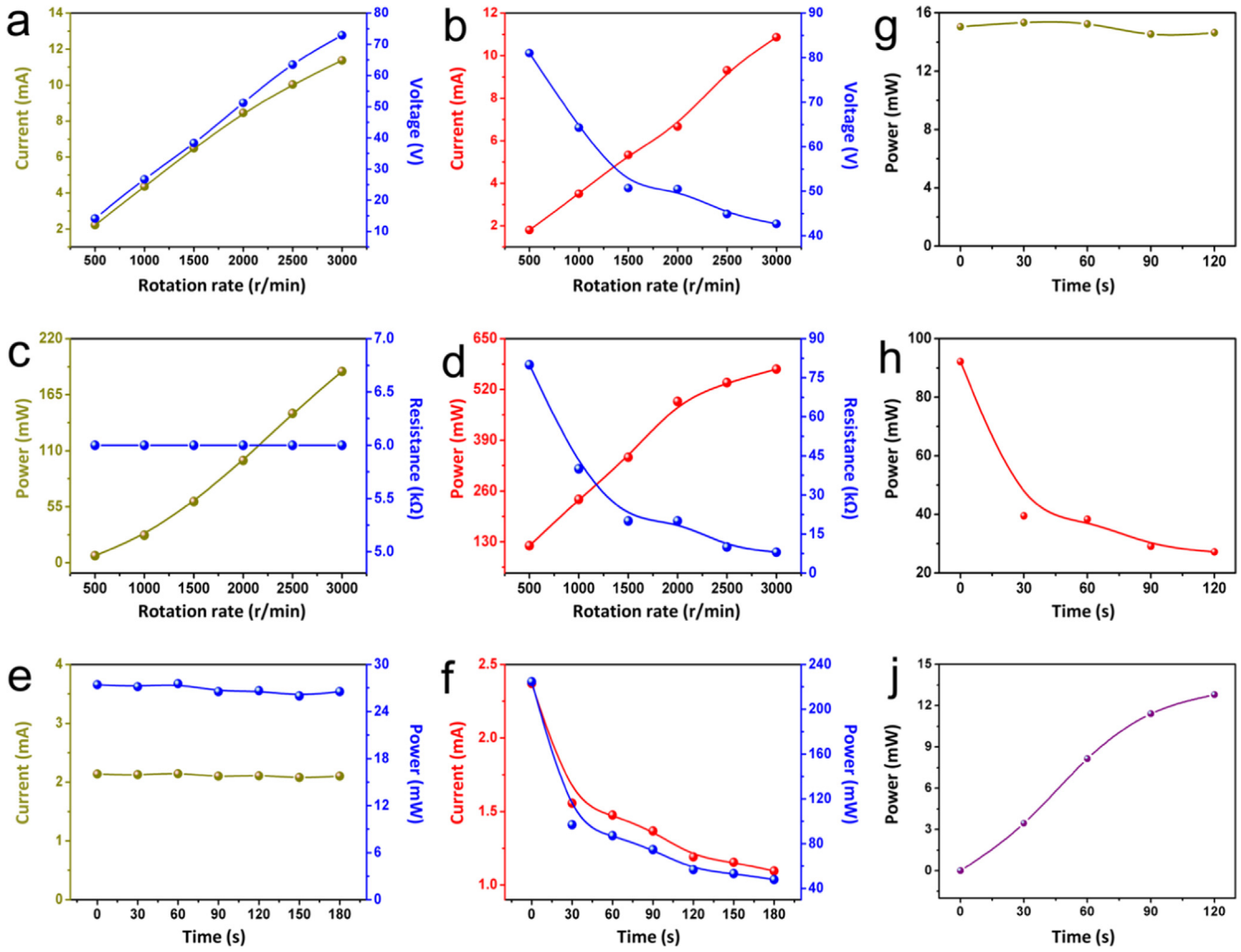

Fig. 4. (a, b) Output current and voltage signals of the EMG (a) and TENG (b) under the different rotation speeds. (c, d) Output powers and the corresponding impedances of the EMG (c) and TENG (d) under the different rotation speeds. (e, f) Output currents and the corresponding powers of the EMG (e) and TENG (f) with increasing the working time. The loading resistances of the EMG and the TENG are 6 kΩ and 40 kΩ, respectively. (g, h) Calculated average powers of the EMG (g) and TENG (h) under the different working time. (j) Output powers of the ThEG under the different working time.

15 mW, as illustrated in Fig. 4(g). As shown in Fig. 4(h), the corresponding average output power $P_{average}$ of TENG was decreased from 92.2 mW to 27.2 mW with increasing the working time from 0 s to 120 s, where the time difference for the t_1 and t_2 is 15 ms for this calculation. Fig. 4(j) depicts the output powers of the ThEG under the different working times, showing a clear increase from 0 mW to 12.8 mW in 120 s.

In the fabricated hybridized nanogenerator, both the EMG and TENG have the AC output signals, while the ThEG has the DC output. To realize that the produced energy can be utilized to directly power some electronic devices or charge a Li-ion battery, all of the output voltages for the EMG, TENG, and ThEG should be same, so that the output current can be enhanced for the hybridized nanogenerator. By using a power management circuit, the output current peak of the EMG can be up to about 162 mA, while the output voltage exhibits a constant DC value of 5 V after 0.4 s, as displayed in Fig. 5(a). Fig. 5(b) shows that the output current peak of the TENG is about 157 mA by using this power management circuit, and the output voltage can be up to 5 V after 0.3 s. Under the same time, the TENG has more output current peaks than that of the EMG, indicating that the TENG can produce more electricity energy than that of the EMG, which is also consistent with the results in Fig. 3. By using another $DC_{low}-DC_{high}$ power management circuit, the output voltage of the ThEG can be up to 5 V in 7.3 s, and the output current of the ThEG after the circuit is about 3 mA when the device was working in 180 s, as depicted in Fig. 5(c). The output voltage of the hybridized nanogenerator can reach 5 V in 0.2 s by integrating the EMG, TENG and ThEG in parallel connections after using the three power management circuits, as displayed in Fig. 5(d). Although the output current peak of the hybridized nanogenerator is still about 160 mA, much more current peaks can be observed in the same time interval than that of the EMG or TENG, as illustrated in Fig. 5(e). Fig. 5(f) displays that the total output current of the hybridized nanogenerator can be up to 208 mA when no power management circuit for ThEG was used, where the number decrease of the output current peaks is due to the output power decrease of the TENG after it was working in several tens of seconds.

To demonstrate the capability of the hybridized nanogenerator as a practical power source for simultaneously scavenging mechanical and thermal energies, the hybridized nanogenerator has been installed in a commercial bicycle. As displayed in Fig. 6(a), the relative rotation motions of two disks can drive the working of the hybridized nanogenerator. As illustrated in Fig. 6(b), the produced energies can be utilized to directly power three globe lights by using the EMG, TENG, and ThEG, respectively. The TENG can

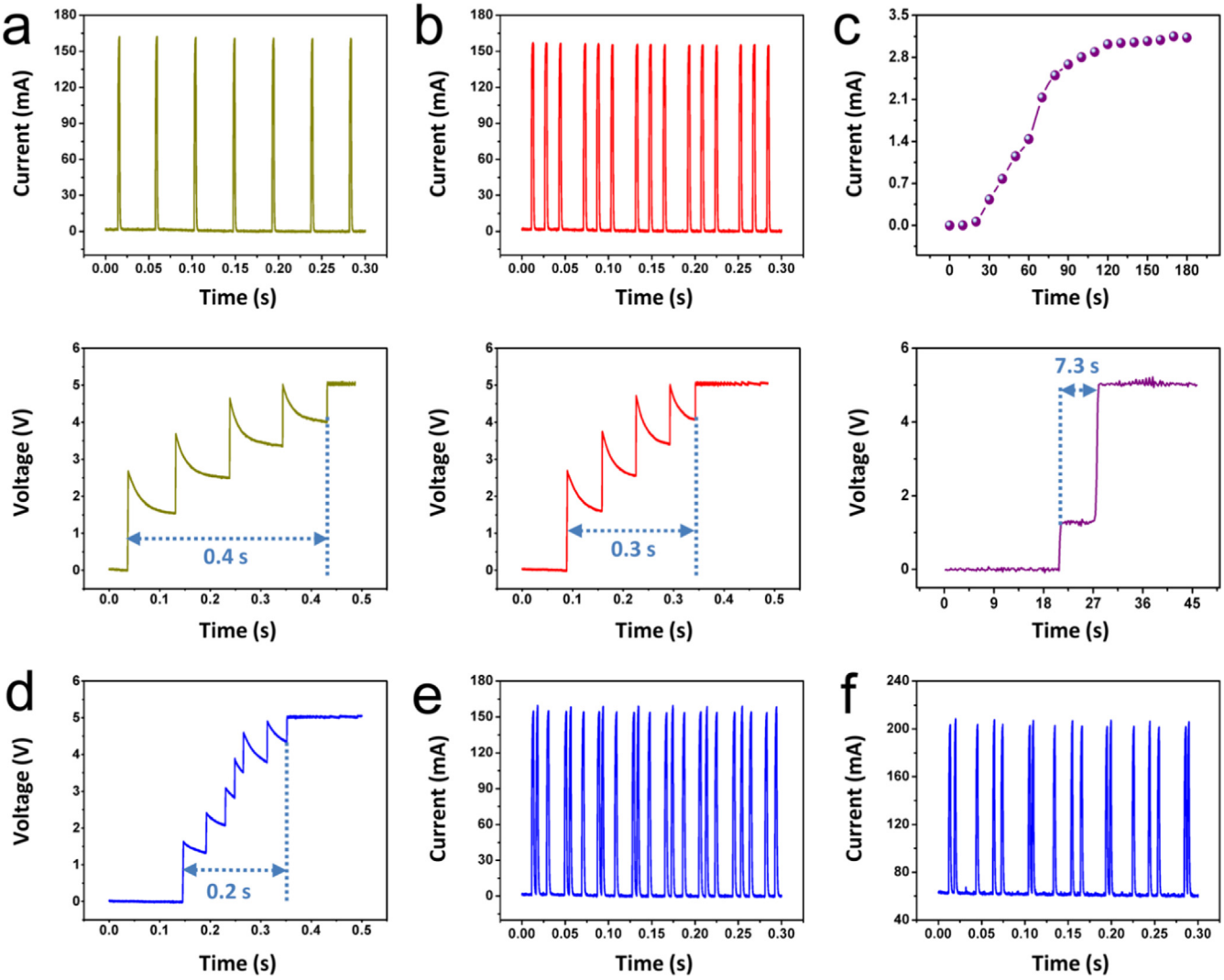

Fig. 5. (a, b, c) Output current and voltage signals of the EMG (a), TENG (b), and ThEG (c) after using the corresponding three power management circuits. (d, e) Output voltage (d) and current (e) signals of the hybridized nanogenerator after using these management circuits. (f) The output current signals of the hybridized nanogenerator after it was working in several tens of seconds, where no management circuit was used for the ThEG.

easily power the globe light under the low rotation speeds, while the EMG can light up the globe light under the relatively higher rotation speeds, as presented in the movie file-1. The ThEG can also power the globe light in a short time after both the EMG and TENG are not working. The hybridized nanogenerator can be also used to charge a cell phone when a person is riding the bicycle, as demonstrated in Fig. 6(c) and the movie file-2. Moreover, a high beam lamp can be also sustainably powered by the hybridized nanogenerator in the bicycle, where the corresponding light density can be up to 1243 lx, which is enough to provide the effective illumination for riding the bicycle at night, as illustrated in Fig. 6(d) and the movie file-3. The demonstrated technology has the potential applications for converting the waste biomechanical energy and the rotation induced thermal energy produced by human riding a bicycle into electricity for solving the power source issues of some electronic devices in the smart bicycles.

As compared with the previous TENG technology, the invented hybridized nanogenerator here has the following advantages: (1) by converting the waste thermal energy in the working process of TENG into electricity, more electric energy can be obtained. (2) By integrating the EMG into the TENG, more electric energy can be produced from the same rotation motions. (3) By hybridizing three energy harvesting units into one device, the hybridized nanogenerator has a much larger output power than that of the individual energy harvesting devices. Among the EMG, TENG and ThEG in the hybridized nanogenerator, the TENG has the largest output power under the same rotation speeds, while its output power can decrease with increasing the working time. In this process, the output power of the EMG keeps a constant value, and a dramatic increase for the output power of the ThEG can be found. Moreover, by using the power management circuits, all of the EMG, TENG and ThEG can deliver a constant DC output voltage of 5 V, which can be utilized to directly power some electronic devices that require a DC power source for maintaining the sustainable operation.

4. Conclusion

In summary, we have fabricated a hybridized nanogenerator that consists of an EMG, a TENG, and a ThEG for simultaneously scavenging mechanical and thermal energies. Both the EMG and the TENG are utilized to harvest the mechanical energy by the relative rotation motions between two disks, and the ThEG can be

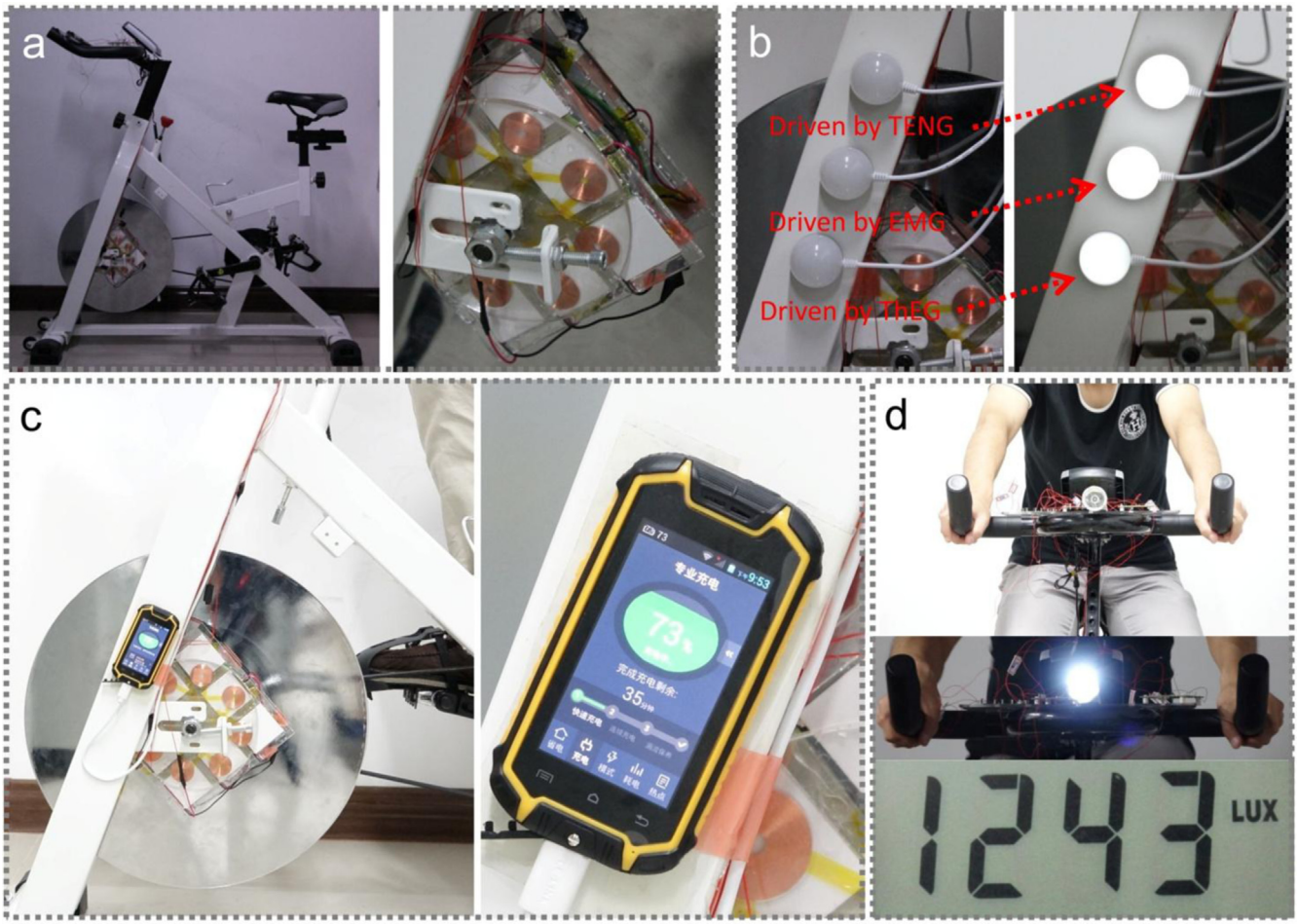

Fig. 6. (a) Photograph of the hybridized nanogenerator installed in a commercial bicycle. (b) Photographs of three globe lights that were directly lighted up by the EMG, TENG and ThEG after using the management circuits, respectively. (c) Photograph of a cell phone that was charged by the hybridized nanogenerator in the bicycle. (d) Photograph of a high beam lamp that can be powered by the hybridized nanogenerator when a person was riding the bicycle, where the corresponding illumination intensity of the lamp is up to 1243 lx.

used to scavenge the triboelectric effect-induced waste thermal energy. The three different energy harvesting units have the different output characteristics with increasing the working time (no change for the EMG, a dramatic decrease for the TENG, an obvious increase for the ThEG). By using the management circuits, the hybridized nanogenerator can deliver a constant output voltage of 5 V and a pulsed output current peak of about 160 mA. We also demonstrated that the fabricated hybridized nanogenerator can be installed in a commercial bicycle to scavenge the waste biomechanical energy from a person riding the bicycle, which can provide an ideal solution for the power source issues of some electronic devices in the smart bicycles.

Acknowledgments

This work was supported by Beijing Natural Science Foundation (2154059), the National Natural Science Foundation of China (Grant nos. 51472055, 61404034), the External Cooperation Program of BIC, Chinese Academy of Sciences (Grant no. 121411KYS820150028), the “thousands talents” program for the pioneer researcher and his innovation team, China. The corresponding patent based on the hybridized nanogenerator and the applications on the bicycle has been filed.

References

[1] D. Fairless, Nature 447 (2007) 1046–1048.
[2] S. Chu, A. Majumdar, Nature 488 (2012) 294–303.
[3] T. Parker, Nature 480 (2011) 315–316.
[4] L.C. Rome, L. Flynn, E.M. Goldman, T.D. Yoo, Science 309 (2005) 1725–1728.
[5] J.M. Donelan, Q. Li, V. Naing, J.A. Hoffer, D.J. Weber, A.D. Kuo, Science 319 (2008) 807–810.
[6] J. Chun, K.Y. Lee, C.-Y. Kang, M.W. Kim, S.-W. Kim, J.M. Baik, Adv. Funct. Mater. 24 (2014) 2038–2043.
[7] S.N. Cha, J.-S. Seo, S.M. Kim, H.J. Kim, Y.J. Park, S.-W. Kim, J.M. Kim, Adv. Mater. 22 (2010) 4726–4730.
[8] C.K. Jeong, J. Lee, S. Han, J. Ryu, G.-T. Hwang, D.Y. Park, J.H. Park, S.S. Lee, M. Byun, S.H. Ko, K.J. Lee, Adv. Mater. 27 (2015) 2866–2875.
[9] F.-R. Fan, Z.-Q. Tian, Z.L. Wang, Nano Energy 1 (2012) 328–334.
[10] B. Meng, W. Tang, Z.-H. Too, X. Zhang, M. Han, W. Liu, H. Zhang, Energy Environ. Sci. 6 (2013) 3235–3240.
[11] J. Chun, J.W. Kim, W.-S. Jung, C.-Y. Kang, S.-W. Kim, Z.L. Wang, J.M. Baik, Energy Environ. Sci. 8 (2015) 3006–3012.
[12] C. Zhang, W. Tang, C. Han, F. Fan, Z.L. Wang, Adv. Mater. 26 (2014) 3580–3591.
[13] Y. Hu, J. Yang, S. Niu, W. Wu, Z.L. Wang, ACS Nano 8 (2014) 7442–7450.
[14] X. Zhong, Y. Yang, X. Wang, Z.L. Wang, Nano Energy 13 (2015) 771–780.
[15] L. Zhang, B. Zhang, J. Chen, L. Jin, W. Deng, J. Tang, H. Zhang, Hong Pan, M. Zhu, W. Yang, Z.L. Wang, Adv. Mater. 28 (2016) 1650–1656.
[16] L. Zhang, L. Jin, B. Zhang, W. Deng, H. Pan, J. Tang, M. Zhu, W. Yang, Nano Energy 16 (2015) 516–523.
[17] C. Han, C. Zhang, W. Tang, X. Li, Z.L. Wang, Nano Res. 8 (2015) 722–730.
[18] Y. Zi, L. Lin, J. Wang, S. Wang, J. Chen, X. Fan, P.-K. Yang, F. Yi, Z.L. Wang, Adv. Mater. 27 (2015) 2340–2347.
[19] H. Guo, Z. Wen, Y. Zi, M.-H. Yeh, J. Wang, L. Zhu, C. Hu, Z.L. Wang, Adv. Energy Mater. 6 (2016) 1501593.

Xue Wang is a M.E. candidate in the research group of Ya Yang at Beijing Institute of Nanoenergy and Nanosystem. His research interest mainly focus on hybrid nanoenergy cells and the applications for some personal electronic devices, and some novel applications.

Zhong Lin (ZL) Wang received his Ph.D. from Arizona State University in physics. He now is the Hightower Chair in Materials Science and Engineering, Regents' Professor, Engineering Distinguished Professor and Director, Center for Nanostructure Characterization, at Georgia Tech. Dr. Wang has made original and innovative contributions to the synthesis, discovery, characterization and understanding fundamental physical properties of oxide nanobelts and nanowires, as well as applications of nanowires in energy sciences, electronics, optoelectronics and biological science. His discovery and breakthroughs in developing nanogenerators established the principle and technological roadmap for harvesting mechanical energy from the environment and biological systems for powering a personal electronics. His research on self-powered nanosystems has inspired the worldwide effort in academia and industry for studying energy of or micro- nano-systems, which is now a distinct disciplinary in energy research and future sensor networks. He coined and pioneered the field of piezotronics and piezo-phototronics by introducing piezoelectric potential gated charge transport process in fabricating new electronic and optoelectronic devices. Details can be found at: http://www.nanoscience.gatech.edu.

Ya Yang received his Ph.D. in Materials Science and Engineering from University of Science and Technology Beijing, China. He is currently a research scientist at Beijing Institute of Nanoenergy and Nanosystems, CAS. His main research interests focus on the field of pyroelectric, piezoelectric, triboelectric, and thermoelectric nanogenerators for energy conversion, storage and some novel applications.